CONF-780941--2

LA-UR-78-2102

TITLE: Vaporization Thermodynamics and Kinetics of Hexagonal Silicon Carbide*

AUTHOR(S): Robert G. Behrens and Gary H. Rinehart

SUBMITTED TO: To be presented at the 10th Materials Research Symposium on the Characterization of High Temperature Vapors and Cases, 18-22 September 1978, at Gaithersburg, Maryland, and to be published in the Symposium Proceedings

los alamos
scientific laboratory
of the University of California
LOS ALAMOS, NEW MEXICO 87545

An Affirmative Action/Equal Opportunity Employer

Form No. 836
St. No. 2629
1/75

UNITED STATES
ENERGY RESEARCH AND
DEVELOPMENT ADMINISTRATION
CONTRACT W-7405-ENG. 36

Vaporization Thermodynamics and Kinetics of Hexagonal Silicon Carbide

Robert G. Behrens and Gary N. Rinehart
University of California
Los Alamos Scientific Laboratory
Los Alamos, New Mexico 87545

Abstract

Mass spectrometer Knudsen effusion vaporization measurements over the temperature range 1835-2264K confirm earlier mass spectrometer results that Si(g) is the predominant vapor species above the SiC-C two-phase region. $Si_2C(g)$ and $SiC_2(g)$ are found to be the next most important vapor species.

Total vapor pressures are measured to be a factor of 10-15 higher than values previously reported between 1800-2200K. Silicon partial pressures lead to a value of -7.5 kcal mol^{-1} for the enthalpy of formation of SiC(hexagonal) at 298K. Partial pressures of Si(g), $SiC_2(g)$, and $Si_2C(g)$ lead to third-law enthalpies of formation for $SiC_2(g)$ and $Si_2C(g)$ which are in accord with previously recommended values.

Langmuir vaporization of SiC(hexagonal) (0001) single crystal faces in the mass spectrometer show ion intensities of Si^+ and SiC_2^+ that are time-independent after an initial induction period during which the intensities increase by a factor of 1.5 before attaining a steady-state value. The mass spectrometer studies between 2200-2500K give activation enthalpies of $\Delta H^*(2350) = 141.6 \pm 2.7$ kcal mol^{-1} for Si(g) and $\Delta H^*(2350) = 166.2 \pm 3.5$ kcal mol^{-1} for $SiC_2(g)$ vaporization from the (0001) crystal face of hexagonal SiC.

Constant temperature total mass-loss Langmuir vaporization experiments using SiC (0001) crystal faces show a time-dependent rate of mass-loss. It is believed that this time-dependent behavior is caused by a decrease in the SiC(hexagonal) single crystal surface area and is not due to impedance of silicon vaporization by the graphite layer formed on the crystal surface during decomposition.

Vaporization Thermodynamics and Kinetics of Hexagonal Silicon Carbide*

Robert C. Behrens and Gary H. Rinehart
University of California
Los Alamos Scientific Laboratory
Los Alamos, New Mexico 87545

1. Introduction

Low atomic number ceramic solids have numerous potential uses in controlled thermonuclear reactor engineering applications.(1-3) Ceramic materials being considered for such applications include SiC, Be_2C, B_4C, BN, Si_3N_4, Al_2O_3, and BeO. These materials are also of interest from a fundamental point of view as many of them vaporize by incongruent decomposition, often yield complex and unique vapor molecules at high temperatures, and are believed to exhibit vacuum vaporization rates lower than the equilibrium values.

The present paper reports the results of investigations on the vaporization thermodynamics of hexagonal silicon carbide using high temperature quadrupole mass spectrometry. Preliminary results of investigations using mass spectrometry to study the vaporization of hexagonal SiC single crystals are also reported. The vaporization thermodynamics and kinetics of hexagonal SiC were investigated because:

1. of the potential application of SiC as a first wall protective barrier in fusion reactors
2. discrepancies exist in the literature regarding the vaporization thermodynamics of SiC and the composition of the equilibrium vapor
3. the vaporization kinetics of SiC have not been previously established
4. single crystal wafers of hexagonal SiC can be readily obtained.

2. Summary of Previous Work on SiC

Silicon carbide, SiC, is believed to be the only compound formed in the Si-C system.(4,5) SiC exists as two phases: an alpha or hexagonal phase and a beta or cubic phase. Cubic SiC is believed to be the thermodynamically stable phase at low temperatures. The cubic to hexagonal phase transition temperature is reported to lie between 2000-2300K.(6) Thermodynamic stabilities of the two SiC phases are believed to be similar, their free energies of formation differing by about 0.5 kcal mol^{-1} at 298K. Hexagonal SiC forms numerous polytypic modifications which arise from different stacking sequences of the hexagonal SiC layers.(7) Differences in the thermodynamic stabilities of these polytypes have not been determined.

*Work performed under the auspices of the Department of Energy

Quantitative data regarding the composition range over which SiC exists have not been reported. It is generally assumed that SiC exists as a line compound.(.)

SiC vaporizes incongruently to form solid graphite as a reaction product. Vapor pressures in both the Si-C and Si-SiC systems have been investigated since as early as 1926. Ruff and Konschak (8) and Ruff and Grieger(9) measured the vapor pressure of the SiC-C system between 1973-2990K and 2565-2951K respectively. Assuming the vapor to consist of Si(g) and SiC(g), these authors were able to calculate Si(g) partial pressures for the SiC-C system.

Drowart, DeMaria, and Inghram (10) used mass spectrometry to establish the vapor composition in the SiC-C system between 2140-2710K. They determined that Si(g) is the predominant vapor species with $SiC_2(g)$ and $Si_2C(g)$ being the next most predominant vapor species over their experimental temperature range. They also found $Si_2(g)$, SiC(g), $Si_2C_2(g)$, $Si_3(g)$, $Si_2C_3(g)$, and $Si_3C(g)$ to be minor species in the equilibrium vapor.

While investigating the spectroscopy of SiC molecules by matrix isolation spectroscopy, Weltner and McLeod (11) found a relatively strong Si_2C_3 spectrum. As they could not determine whether the strong spectrum was due to a high transition probability of the Si_2C_3 bands in the visible region of the spectrum or to a concentration of Si_2C_3 in the SiC-C vapor higher than that suggested by the mass spectrometry results of Drowart et al., Weltner and McLeod suggested that the importance of this molecule in the high temperature equilibrium vapor of SiC-C be re-examined.

Knippenberg (5) measured the total vapor pressure of hexagonal SiC in a graphite crucible and determined the silicon content of the vapor at the normal sublimation temperature (3037K from Knippenberg's work). On the basis of his analysis, Knippenberg concluded that the equilibrium gas phase composition of the SiC-C system is always rich in silicon in contrast to the results of the mass spectrometer studies of Drowart et al. which indicate the Si/C ratios in the gas phase to be less than unity.

Drowart and DeMaria (12) measured the vapor pressure of the Si-SiC system using mass spectrometry and found Si(g) to be the major vapor species with $Si_2C(g)$ and $SiC_2(g)$ being the next most important vapor species below 2632K. Enthalpies of formation of $Si_2C(g)$ and $SiC_2(g)$ calculated by a third-law analysis of the vapor pressure data are consistent with the corresponding third-law values from Drowart et al's mass spectrometer work on SiC-C. Total vapor pressures extrapolated to the temperature range over which Ruff and co-workers(8,9) measured total vapor pressures of the Si-SiC system are in poor agreement with Ruff's results. Drowart and DeMaria attributed this discrepancy to the fact that silicon diffused through the crucible in Ruff's experiments causing their vapor pressures to be inordinately high.

Grieveson and Alcock (13) used a mass-loss effusion technique to measure the total vapor pressure of both hexagonal and cubic SiC. The measured total vapor pressures for each SiC phase were slightly higher than those reported by Drowart et al. At temperatures above 1973K, Grieveson and Alcock found that their vapor pressures for hexagonal SiC were higher than values calculated by extrapolating their low temperature data. This behavior may indicate that the low temperature vapor pressures are too low because of kinetic problems (ie. a low vaporization coefficient).

Davis, Anthrop, and Searcy (14) measured the vapor pressures of cubic SiC by a mass-loss effusion technique using Drowart et al's mass spectrometer results to calculate Si(g) partial pressures from their observed mass losses. They obtained total vapor pressures in agreement with the total vapor pressures measured by Grieveson and Alcock. Davis et al. also report that they found no systematic change

in the vapor pressure as a function of cell orifice area and concluded that the vaporization coefficient of Si(g) from cubic SiC was close to unity. They did, however, observe a time-dependent decrease in the vaporization rate which they attributed to impedance of Si(g) vaporization by a graphite microlayer formed on the SiC particles during vaporization.

Mell and Brodsky (15) obtained the mass spectrum of silicon evaporating from a carbon-lined copper hearth under high vacuum (the temperature at which the mass spectrum was taken was not reported). They observed peaks for most of the known Si-C and Si molecules but did not observe a peak attributable to $SiC_2(g)$.

Mass-loss effusion studies of SiC-C by Voronin, Makarova, and Yudin (16) give vapor pressures which are a factor of 20-30 below those of the previously discussed investigations. These results indicate a low vaporization coefficient in contradiction to the results of Davis et al. Ghoshtagore (17) performed Langmuir vaporization experiments using hexagonal SiC single crystal wafers and reported vaporization rates a factor of 10^4 lower than those measured under equilibrium conditions.

3. Experimental Section

A. Sample Characterization

Knudsen effusion experiments are performed using 200 mesh SiC particles, 200 mesh SiC particles crushed to 325 mesh powder, or 325 mesh SiC powder mixed with 325 mesh H-451 reactor grade graphite powder. X-ray diffraction shows the SiC to be the hexagonal phase, most probably a mixture of polytypes. Cubic SiC may also be present as X-ray diffraction lines for the cubic phase are not clearly discernible from those for the hexagonal phase. The X-ray diffraction patterns also show that significant amounts of impurities are not present in the SiC samples.

Langmuir vaporization experiments are performed using hexagonal SiC single crystal wafers purchased from the Materials Research Corporation, Orangeburg, N.Y.. The crystals are carbon arc grown, 6-8 mm in cross-section, and 1 mm thick with the c-axis oriented perpendicular to the large face. X-ray diffractometer scans confirm the crystals to be hexagonal SiC.

B. Experimental Apparatus

The mass spectrometer used for both the Knudsen effusion and Langmuir vaporization experiments is shown in Figures 1 and 2. The mass spectrometer consists of an Extranuclear Laboratories field separation (ELFS) quadrupole mass filter. The quadrupole rods are 0.95 cm diameter by 20 cm long giving a mass range of 1400 amu with a resolution of approximately 1000 at m/e = 1000.

The electron impact ionizer is of cross-beam design, that is, the molecular beam from the high temperature source enters the ionizer region in a direction normal to the geometrical axis of the quadrupole rods and normal to the direction of ion extraction into the mass filter.

Ion detection is achieved by a 21-stage copper-beryllium "Venetian blind" electron multiplier mounted paraxial to and offset from the quadrupole transmission axis. Multiplier gains are determined in the usual manner using a Faraday plate detector.

Multiplied ion currents pass through a preamplifier, through a 10^7 or 10^9 ohm resistor, and into a dc electrometer. Output from the electrometer is displayed on an oscilloscope, X-Y recorder, or a strip chart recorder.

The electron multiplier-mass filter-ionizer assembly is mounted as a single unit on an 8-inch o.d. Conflat flange through which electrical connections to the quadrupole power supply, ionizer control, and electrometer are made. The assembly is mounted horizontally on a 5.5-inch i.d. stainless steel bellows which can be adjusted to permit easy alignment of the ion source entrance hole with the molecular beam from the high temperature Knudsen cell region. (See Figure 1)

The vacuum system is constructed entirely of 6-inch o.d. stainless steel tubing. Conflat flanges with copper gaskets are used in all vacuum connections. A Varian HC-12E vacuum station is used to pump on the ion source region. The station consists of 200 l s^{-1} of Triode VacIon pumping, a titanium sublimation pump (TSP), and a liquid nitrogen cryoarray. A peppet valve is located above the VacIon pumps and TSP to permit breaking of vacuum without turning off the pumps. Pumping of the Knudsen cell region is achieved by a 400 l s^{-1} Thermionics Laboratory VacIon pump. Rough pumping of the system is achieved by three liquid nitrogen-cooled VacSorb pumps. These pumps are isolated from the main vacuum system by 1.5-inch polyimide-sealed ultra-high vacuum valves (See Figure 2).

Typical background pressures of 5×10^{-9} torr are readily achieved in both the ion source and Knudsen cell regions after about six hours pumping from 10 microns pressure. Background pressures on the order of 1×10^{-7} torr or better in the ion source region and 1×10^{-6} torr or better in the Knudsen cell region are routinely achieved during operation with a graphite Knudsen cell at temperatures as high as 2300K.

The Knudsen cell region is separated from the ion source region of the mass spectrometer by a water-cooled plate with a 0.25-inch diameter hole through its center. A stainless steel shutter blade with a 0.025-inch wide slit sloxed into it rests on top of the water-cooled plate and is moved across the path of the molecular beam from the Knudsen cell region by a linear-motion vacuum feedthrough.

A graphite Knudsen effusion cell or SiC single crystal situated in a graphite holder is heated by a tungsten spiral resistance heater mounted on an 8-inch o.d. Conflat flange (Figure 3). A Sorenson high current, low voltage dc power supply is used to supply power to the tungsten heater. Water-cooled copper power feedthroughs for the tungsten heater are brought into the vacuum system through the 8-inch o.d. flange. A concentric arrangement of six tantalum and two tungsten shield cans, with molecular beam exit holes drilled through the center of their tops, is situated around the tungsten heater. Seven tantalum heat shields, with pyrometer sight holes drilled through their centers, are situated directly below the heater. The entire furnace arrangement fits into a 6-inch o.d. stainless steel housing which has 0.25-inch o.d. copper tubing brazed to the outside wall for water cooling.

The temperature of a Knudsen cell is measured using a calibrated Pyro optical pyrometer by sighting through an optical window onto a blackbody hole drilled into the bottom of the Knudsen cell. Single crystal temperatures are measured by sighting the pyrometer through a hole drilled in the bottom of a cylindrical graphite holder onto the underside of the single crystal. Observed temperatures are then corrected for optical window and prism effects.

Knudsen effusion cells used in the equilibrium vapor pressure measurements are machined from graphite and are of two types. The first type consists of a base with a lid, has a 1.3 cm outside diameter and is approximately 1.8 cm long. The cell lid contains a knife-edge circular orifice with an area of 3.0×10^{-3} cm^2 and a Clausing factor of 0.502. The second type of Knudsen effusion cell consists of a single piece of graphite 1.8 cm in length and 1.3 cm in outside diameter. A 0.48 cm long graphite plug with a cylindrical hole drilled through its center provides the orifice. The orifice area is 0.027 cm^2 with a Clausing factor of 0.385.

Total mass-loss Langmuir vaporization experiments are performed with an SiC single crystal wafer sitting in a graphite holder. The crystal and holder are seated in the center of a water-cooled eddy-current concentrator on a Veeco vacuum pumping system. The current concentrator is coupled to induction coils from a Lepel 20 kW induction heating unit. The crystal surface temperature is measured by sighting a Pyro optical pyrometer through a quartz window located at the top of the concentrator onto the crystal surface. The mass change of the crystal after heating for a given time period is determined by removing the crystal from the concentrator and weighing it on a Mettler pan micro-balance.

C. Data Treatment

Ion intensities from the SiC Knudsen effusion studies are converted to absolute partial pressures for each vapor species assuming the ion transmission efficiency of the mass filter is independent of m/e; using the results of a separate Knudsen effusion vaporization of gold from a graphite crucible, and using the relation

$$(1) \qquad P_u = C_{Au} \frac{I T (\sigma \gamma f i)_{Au}}{(\sigma \gamma f i)_u}$$

where P_u is the pressure of molecular species u with measured ion intensity I_u ; C_{Au} is the instrument sensitivity; T is the thermodynamic temperature; γ is the electron multiplier gain; f is the isotopic abundance; i is an emission current correction factor; and σ is the calculated ionization cross-section at the working electron energy. The instrument sensitivity, C_{Au}, is obtained from the gold vaporization experiment and the known vapor pressure of gold.(18)

Vapor pressures obtained using equation (1) are fitted to the relation

$$(2) \qquad R \ln(P/atm) = -\Delta H^\circ/T + \Delta S^\circ$$

by a least-squares calculation. Second-law values of $\Delta H^\circ(298)$ and $\Delta S^\circ(298)$ are calculated by a Σ' evaluation of the vapor pressures.(19) Third-law values of $\Delta H^\circ(298)$ are obtained in the usual manner.(20)

Time-independent ion intensities from the single crystal Langmuir vaporization studies are fitted to the relation

$$(3) \qquad R \ln(IT) = -\Delta H^*/T + \text{Constant}$$

by a least-squares calculation. The quantity ΔH^* is the activation enthalpy change for the vaporization process. The similar form of equations (2) and (3) permits

ΔH^* and ΔH^o to be compared to yield an enthalpy barrier, $\Delta H^* - \Delta H^o$, for the kinetically slow step(s) in the vaporization process.

4. Experimental Results

A. Knudsen Effusion Mass Spectrometer Measurements on the SiC-C System

The most important vapor molecule in the SiC-C system over the experimental temperature range of 1835-2264K is found to be Si(g) with SiC_2(g) and Si_2C(g) being the next most important molecules. Only trace amounts of detectable Si_2(g), Si_2C_2(g), Si_3(g), and Si_3C(g) are detected to be present at 2275K. Mass spectrum peaks attributable to ions of other silicon or silicon-carbon molecules are not detected. These results are in accord with the mass spectrometer results of Drowart et al.(10). X-ray analysis of the solid product remaining after complete vaporization of silicon shows it to be graphite.

Temperature coefficient plots for Si^+(m/e = 28), SiC_2^+(m/e = 52), and Si_2C^+(m/e=68) are shown in Figure 4 for a typical mass spectrometer experiment using a graphite effusion cell with a 3×10^{-3} cm^2 orifice area and 325 mesh SiC powder. For this particular experiment, electron energies of 13 ev are used for the Si^+ intensity measurements and 15 ev for the SiC_2^+ and Si_2C^+ measurements. An emission current of 2.0 mA is used for all the measurements.

Figure 4 shows attenuation of the Si^+, Si_2C^+, and SiC_2^+ intensities at high temperatures. This behavior is believed to be caused by intramolecular scattering in the molecular beam. Ion intensity attenuation caused by intramolecular scattering as predicted by a model developed by Meschi(21,22) is indicated in Figure 4 by the dashed lines. The total vapor pressure inside the SiC-containing graphite Knudsen cell at which attenuation is first observed is in good agreement with that predicted by Meschi's model. However, agreement between the magnitude of the observed attenuation and that predicted by Meschi's model is only qualitative. This discrepancy may be caused by incorrect assumptions contained in the model, incorrect assumptions concerning collision cross-sections for Si-C molecules used in the calculations, or by an added contribution due to scattering of molecules in the molecular beam by background gases.

To assure that the observed ion intensity attenuation is not caused by some anomalous behavior of the mass spectrometer or by vaporization kinetic problems (e.g. solid state diffusion of silicon is determining the vaporization rate at high temperature), vaporization of molten gold from a graphite Knudsen cell was studied at temperatures where the gold vapor pressure is on the order of 10^{-3}-10^{-4} atmospheres. A temperature coefficient plot for this experiment is shown in Figure 5(data are taken using 20 ev electron energy, 3.0 mA emission current). Attenuation of the Au^+ (m/e = 197) intensities starts at gold vapor pressures predicted from Meschi's model (about 5×10^{-4} atmospheres). The magnitude of the attenuation is also comparable to that predicted by the model.

Measured partial pressures of Si(g), SiC_2(g), and Si_2C(g) are found to depend on both the SiC particle size and the size of the Knudsen cell orifice. SiC powder ground to 325 mesh (44 micron) and vaporized from a Knudsen cell with a 3×10^{-3} cm^2 orifice area gives the highest measured vapor pressures. A coarsely crushed hexagonal SiC single crystal vaporized from the crucible with a 3×10^{-3} cm^2 orifice area gives partial pressures 90 percent below vapor pressures obtained with the 325 mesh samples. Vapor pressures measured using 200 mesh SiC powder and a crucible with a 0.027 cm^2 orifice

area are 65 percent lower than those obtained using the 325 mesh powder in an effusion cell with a 3×10^{-3} cm^2 orifice area. Samples of 200 mesh SiC powder vaporized in the effusion cell with an 3×10^{-3} cm^2 orifice area give measured partial pressures the same as obtained with the 325 mesh samples.

Because of the orifice and particle size effects, thermodynamic quantities for SiC vaporization are calculated using data from those experiments with 200 and 325 mesh SiC powder and a 3×10^{-3} cm^2 orifice area. Second- and third-law enthalpies of vaporization at 298K for the reactions

1. $SiC(s) = Si(g) + C(s)$

2. $SiC(s) + C(s) = SiC_2(g)$

3. $2SiC(s) = Si_2C(g) + C(s)$

are summarized in Table 1. These values are obtained as described in Section 3-C and using JANAF(6) free energy functions. Vapor pressures computed using the present third-law enthalpy changes and JANAF free energy functions are given in Table 2.

B. Mass Spectrometer and Total Mass-Loss Langmuir Vaporization Experiments

Two mass spectrometer experiments, performed over the temperature range 2200-2500K, investigated the Langmuir vaporization from the (0001) basal plane of two separate SiC single crystals. Shutterable ions observed are Si^+, SiC_2^+, and Si_2C^+. Ion intensities are found to be independent of time after an initial induction period during which the intensity of Si^+ (and presumably SiC_2^+ and Si_2C^+) increases with time. The steady-state Si^+ intensity is a factor of 1.5 higher than that measured during the initial stages of heating. At 2400K measured steady-state ion intensities are a factor of 80-100 lower than intensities extrapolated from those measured in the Knudsen effusion experiments.

The measured temperature-dependence of Si^+ and SiC_2^+ intensities yield activation enthalpies of $\Delta H^*(2350) = 141.6 \pm 2.7$ kcal mol^{-1} for Si(g) and $\Delta H^*(2350) = 166.2 \pm 3.5$ kcal mol^{-1} for $SiC_2(g)$ sublimation from the (0001) plane of hexagonal SiC. Comparison of these activation enthalpies with the corresponding equilibrium enthalpies obtained in the present work, $\Delta H^o(2350) = 111.3$ kcal mol^{-1} and $\Delta H^o(2350) = 143.7$ kcal mol^{-1}, respectively, gives enthalpy barriers of 30.3 kcal mol^{-1} and 22.5 kcal mol^{-1} for Si(g) and $SiC_2(g)$ sublimation.

Results of a total mass-loss Langmuir vaporization study of the SiC (0001) face are shown for one experiment conducted at 2498K in Figure 6. The results show that the total mass-loss is time-dependent during the entire course of vaporization (i.e. from initial heat-up until all the silicon is vaporized from the crystal). Figure 7 shows the mass-loss data of Figure 6 plotted against $t^{1/2}$ indicating a parabolic time-dependence. Figure 8 shows the time-dependence of the apparent flux vaporizing from the (0001) crystal face calculated from the data shown in Figure 6. It should be noted that the flux measured initially (0.31 mg min^{-1} cm^2) is a factor of about 10^4 below the equilibrium flux of Si(g) at 2498K, and that during the 1300 minute vaporization, the apparent flux drops by a factor of four. The flux then immediately drops to zero at which time it is believed that the silicon is completely depleted from the crystal.

The residue formed on the SiC single crystal substrate was investigated using X-ray diffraction and scanning electron microscopy (SEM). X-ray diffraction scans show the residue to be graphite. Broadening of the 002 and 004 graphite diffraction peaks indicates the graphite surface to be composed of small graphite crystallites. Scanning electron microscopy shows no pores to be present at magnifications of up to 50,000X.

Table 1. Comparison of Vaporization Enthalpies for the SiC(hex)-C System

Reaction	$\Delta H^o(298)$, second-law (kcal mol^{-1})		$\Delta H^o(298)$, third-law (kcal mol^{-1})	
	This Work	Reference 10[a]	This Work	Reference 10[a]
$SiC(s) = Si(g) + C(s)$	114.2±2.1[b]	136.9±0.7[b]	115.2±0.8	124.6±0.3
$2SiC(s) = Si_2C(g) + C(s)$	162.4±2.1	169.6±7.5	145.3±1.2	161.3±0.5
$SiC(s) + C(s) = SiC_2(g)$	169.0±6.4	168.1±9.4	152.1±1.4	163.6±0.6

(a) Recalculated from partial pressures reported in Reference 10 using JANAF free energy functions.
(b) All uncertainties are quoted as one standard deviation.

Table 2. Comparison of Calculated Equilibrium Pressures in the SiC(hex)-C System

Molecule	T(K)	P(atm) This Work[a]	P(atm) Reference 10[a]
Si	1800	1.2×10^{-6}	8.7×10^{-8}
	2000	2.9×10^{-5}	2.7×10^{-6}
	2200	3.8×10^{-4}	4.4×10^{-5}
SiC_2	1800	3.6×10^{-8}	1.5×10^{-9}
	2000	2.3×10^{-6}	1.3×10^{-7}
	2200	6.6×10^{-5}	4.7×10^{-6}
Si_2C	1800	1.2×10^{-7}	1.3×10^{-9}
	2000	5.7×10^{-6}	1.0×10^{-7}
	2200	1.4×10^{-4}	3.5×10^{-6}
P_{total}	1800	1.4×10^{-6}	9.0×10^{-8}
	2000	3.7×10^{-5}	2.9×10^{-6}
	2200	5.9×10^{-4}	5.2×10^{-5}

(a) Calculated using third-law values of $\Delta H^o(298)$ given in Table 1 and JANAF free energy functions.

5. Discussion

A. Knudsen Effusion Mass Spectrometer Experiments

Over the temperature range 1800-2200K equilibrium partial pressures of Si(g), $SiC_2(g)$, and $Si_2C(g)$ above SiC-C measured in the current work are higher than pressures reported by Drowart et al.(10) by factors of 10-15, 15-25, and 40-90 respectively. Accordingly, total vapor pressures of the present work are a factor of 10-15 higher than those of Drowart et al.(10). Present total vapor pressures extrapolated to 2800-2900K are in excellent agreement with total pressures measured at these temperatures by Ruff and Konschak(8) and Ruff and Grieger(9).

Table 1 shows excellent agreement between present second- and third-law values of $\Delta H^0(298)$ for reaction (1). Agreement between second- and third-law enthalpies for reactions (2) and (3) is not good, the second-law enthalpies being 17 kcal mol^{-1} lower than the corresponding third-law values. The reason for this discrepancy is not known. Note, however, that the present second-law enthalpies for reactions (2) and (3) are in good agreement with the corresponding third-law enthalpies reported by Drowart et al.

The enthalpy of formation of SiC(hexagonal) at 298K computed from the present third-law enthalpy change for reaction (1) and the enthalpy of formation for Si(g) given in the JANAF tables, 107.7 kcal mol^{-1} at 298K, is -7.5 kcal mol^{-1}. This value is 9.4 kcal mol^{-1} more positive than that recommended by JANAF. The JANAF value is based on the enthalpy of reaction for SiC(hex) + $4F_2(g)$ = $SiF_4(g)$ + $CF_4(g)$ measured by fluorine bomb calorimetry. However, an accurate enthalpy of formation for SiC measured in this manner depends on accurate enthalpies of formation for $SiF_4(g)$ and $CF_4(g)$. We believe the enthalpy of formation of $SiF_4(g)$ to be sufficiently uncertain so as to raise serious questions regarding the reliability of the JANAF recommended value for the enthalpy of formation of SiC.

Enthalpies of formation for $Si_2C(g)$ and $SiC_2(g)$ are computed to be 130.3 kcal mol^{-1} and 144.6 kcal mol^{-1} respectively using the present third-law enthalpy changes for reactions (1) through (3) given in Table 1. These are in excellent agreement with values recommended by JANAF based on the mass spectrometer results of Drowart et al.(10,12), 128 $\pm$ 6 kcal mol^{-1} and 147 $\pm$ 7 kcal mol^{-1} respectively.

B. Langmuir Vaporization Experiments

Activation enthalpy barriers of 30.3 kcal mol^{-1} for Si(g) and 22.5 kcal mol^{-1} for $SiC_2(g)$ vaporization from the SiC(hexagonal) basal plane lead to vaporization coefficients of 1.5×10^{-3} and 8.1×10^{-3} respectively at 2350K if it is assumed there are no corresponding entropy barriers for the kinetically-slow step in the vaporization process(i.e. $\Delta S^o = \Delta S^*$).

The time-independent Si^+ and SiC_2^+ intensities observed in the mass spectrometer Langmuir single crystal experiments show that the porous graphite layer formed as a result of SiC decomposition has little or no affect on the transport rate of Si(g) and $SiC_2(g)$ from the crystal surface. The parabolic time-dependence of the total mass-loss observed in the mass-loss Langmuir experiments is believed to be due to a decrease in the surface area of the single crystal as decomposition proceeds and not due to a diffusion-controlled rate-limiting step in the vaporization process. A time-dependent decrease in Si^+, SiC_2^+, and Si_2C^+ intensities due to a decrease in the single crystal surface area is not expected to be observed in the Langmuir mass spectrometer experiments as only a small portion of the vapor flux from the center of the SiC crystal surface is sampled by the mass spectrometer.

A simple model used to calculate the mass-loss of a cube with a surface area decreasing with time gives mass-losses in qualitative agreement with those observed

experimentally. The data shown in Figure 6 best fit the model at short times ($t \leq 500$ minutes). At longer times, the model predicts a too-slow decrease in the surface area with time and hence too-fast a loss of material in comparison with the experimental data.

Details concerning the mechanism for the decomposition of SiC cannot be presented at this time. However, on the basis of a model developed by Searcy for endothermic decomposition reactions which form porous solid reaction products, the preliminary vaporization data and SEM results reported here indicate that either a chemically activated mechanism of surface diffusion or a step involving the gaseous reaction products is rate-limiting(24,25).

6. Acknowledgements

We wish to thank Alan Searcy for helpful discussions concerning the kinetics of decomposition reactions and for informing us of Meschi's model for intramolecular scattering; MaryAnn David for performing some of the mass spectrometer Knudsen effusion measurements; and Terry Wallace for his support and interest in this project. We wish also to thank the Los Alamos Scientific Laboratory for providing funds under its New Research Initiatives Program.

7. References

1. L. H. Rovner and G. R. Hopkins, Nuclear Tech. 29, 274(1976).

2. G. R. Hopkins "Low Atomic Number Materials for Fusion. An Assessment Study", General Atomic Company report GA-A13306(September 15, 1974).

3. C. J. McHargue and J. L. Scott, Metall. Trans. A, 9A, 151 (1978).

4. R. I. Scace and G. A. Slack, J. Chem. Phys. 30, 1551 (1959).

5. W. F. Knippenberg, Philips Research Reports 18, 161(1963).

6. D. R. Stull and H. Prophet, JANAF Thermochemical Tables, Second edition, National Bureau of Standards publication NSRDS-NBS 37 (June 1971).

7. A. Addamiano, "Speculations on the Origins of the Polytypism of SiC" In Silicon Carbide-1973, p. 179, Univ. of S. Carolina Press, Columbia, S.C. (1973).

8. O. Ruff and M. Konschak, Z. Electrochem. 32, 515 (1926).

9. O. Ruff, Trans. Electrochem. Soc. 68, 87 (1935).

10. J. Drowart, G. DeMaria, and M. G. Inghram, J. Chem. Phys. 29, 1015 (1958).

11. W. Weltner, Jr. and D. McLeod, Jr., J. Chem. Phys. 41, 235 (1964).

12. J. Drowart and G. DeMaria, "Thermodynamic Study of the Binary System Carbon-Silicon Using a Mass Spectrometer", In Silicon Carbide. A High Temperature Semiconductor, J. R. O'Connor and J. Smiltens, editors, Pergamon Press, p.16 (1960).

13. P. Grieveson and C. B. Alcock, "The Thermodynamics of Metal Silicides and Silicon Carbide", in Special Ceramics, P. Popper, editor, Heywood and Company Ltd., London, p. 183 (1960).

14. S. G. Davis, D. F. Anthrop, and A. W. Searcy, J. Chem. Phys. 34, 659 (1961).

15. H. Mell and M. H. Brodsky, Thin Film Solids 46, 299 (1977).

16. N. I. Voronin, N. L. Makarova, and B. F. Yudin , Issled. v Obl. Khim. Silikatov i Oksidov, Akad. Nauk SSSR, Sb. Statei 1965, 203.

17. R. N. Ghoshtagore, Solid-State Electronics 9, 178 (1966).

18. R. C. Paule and J. Mandel "Analysis of Interlaboratory Measurements on the Vapor Pressure of Gold", National Bureau of Standards Special Publication 260-19 (January, 1970).

19. D. Cubicciotti, J. Phys. Chem. 70, 2410 (1966).

20. R. G. Behrens and G. M. Rosenblatt, J. Chem. Thermodynamics 4, 175 (1972).

21. D. Meschi, J. Phys. Chem. 76, 2947 (1972).

22. J. Roberts, Jr. and A. W. Searcy, High Temperature Science 4, 411 (1972).

23. E. Groenberg, C. A. Natke, W. N. Hubbard, J. Chem. Thermodynamics 2, 193 (1970).

24. A. W. Searcy and D. Beruto, J. Phys. Chem. 80, 425 (1976).

25. A. W. Searcy and D. Beruto, J. Phys. Chem. 82, 163 (1978).

Figure Captions

Figure 1. High temperature mass spectrometer. View 1.

Figure 2. High temperature mass spectrometer. View 2.

Figure 3. Tungsten spiral resistance heater on 8-inch Conflat flange.

Figure 4. Temperature coefficient plot of Si^+, SiC_2^+, and Si_2C^+ for a typical mass spectrometer Knudsen effusion experiment using a graphite effusion cell with 3×10^{-3} cm^2 orifice area. Dashed lines indicate expected intensity attenuation calculated using Hoshi's model for intramolecular scattering(Ref. 21).

Figure 5. Temperature coefficient plot of Au^+ data from mass spectrometer Knudsen effusion experiment using a graphite effusion cell with 3×10^{-3} cm^2 orifice area.

Figure 6. Time-dependence of total mass-loss from a freely vaporizing hexagonal SiC (0001) single crystal face at 2498K.

Figure 7. Total mass-loss data of Figure 6 showing parabolic time-dependence.

Figure 8. Time-dependence of total flux vaporizing from the (0001) SiC single crystal face at 2498K. Calculated from data in Figure 6.

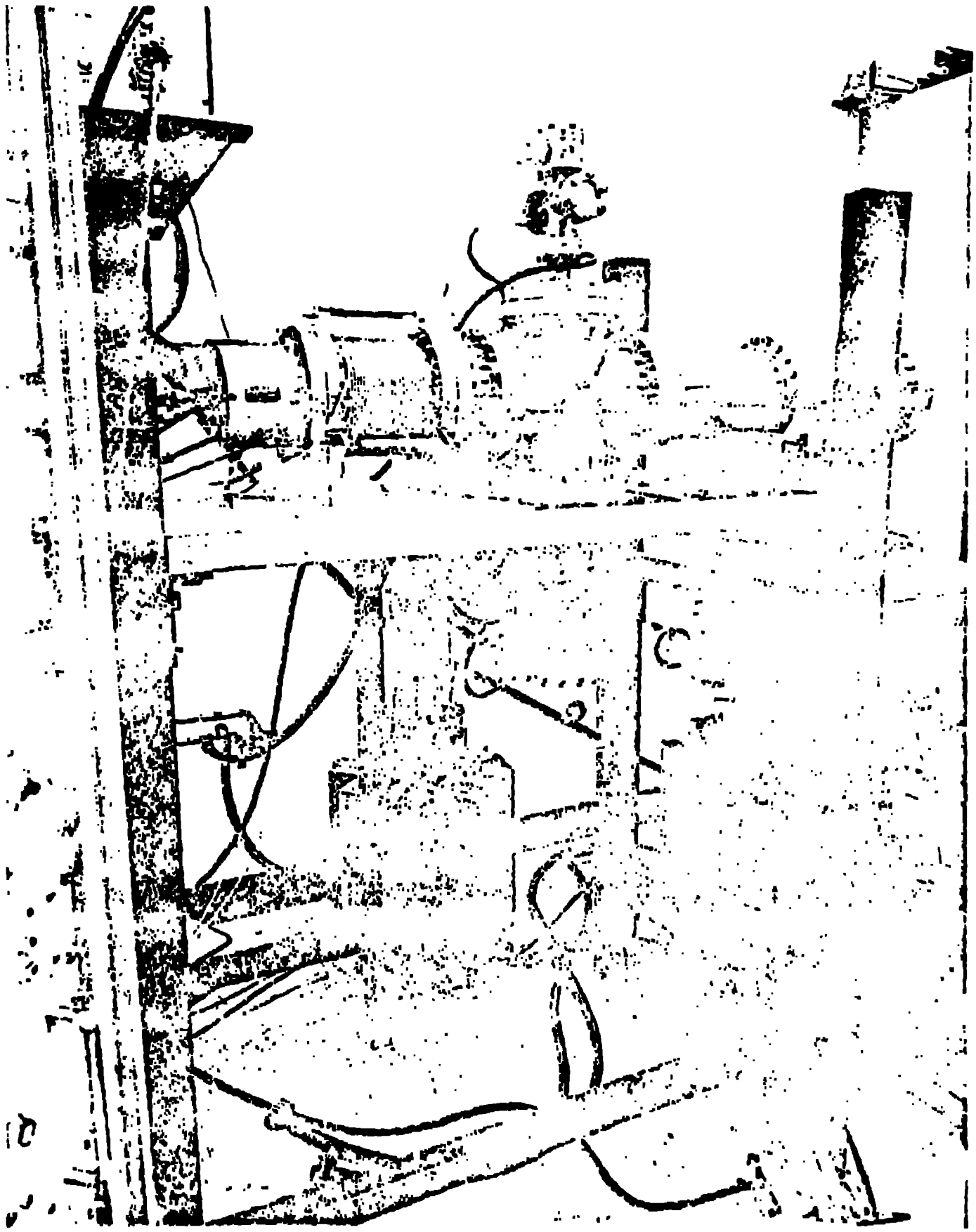

Figure 1. High temperature mass spectrometer. View 1.

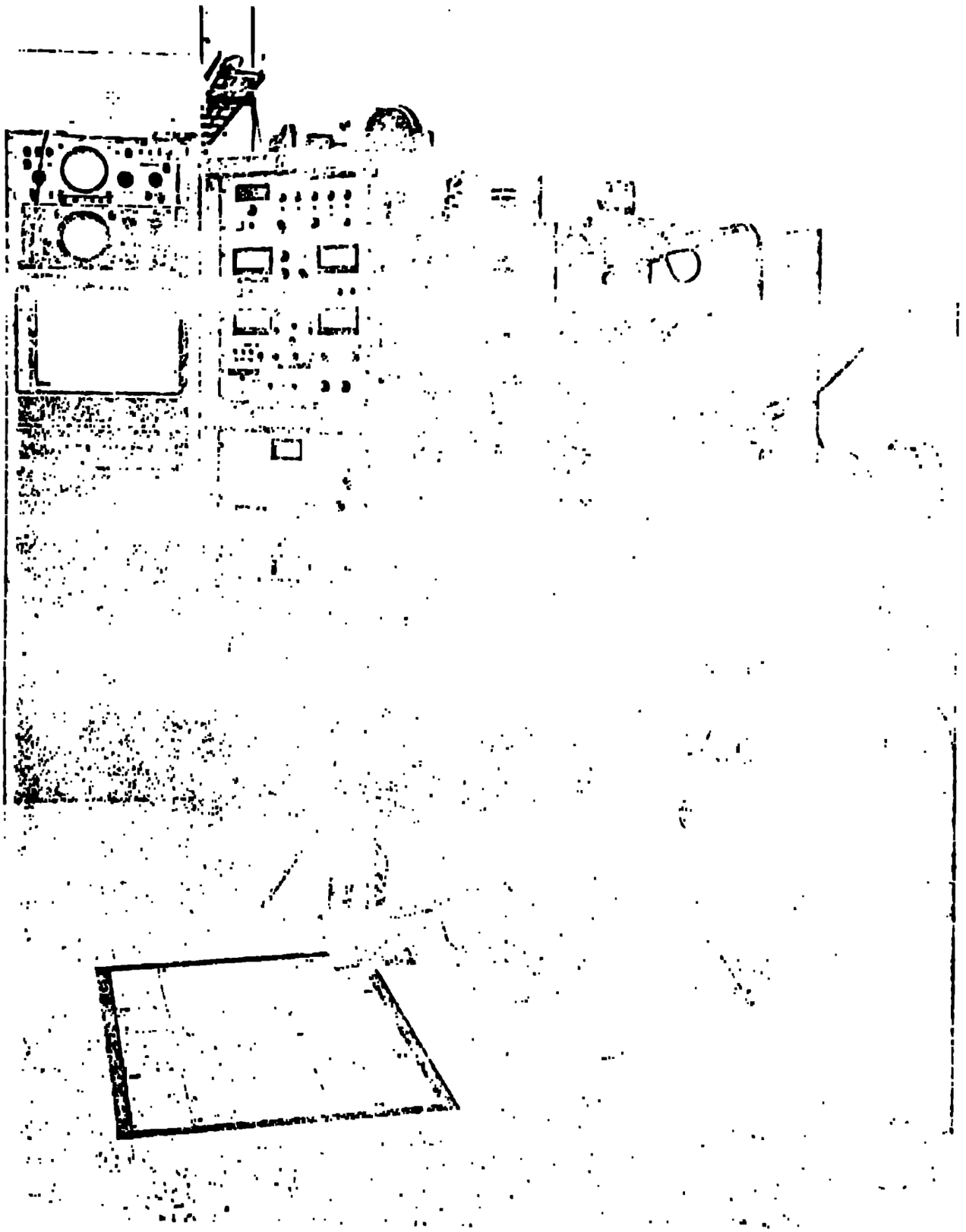

Figure 2. High temperature mass spectrometer. View 2.

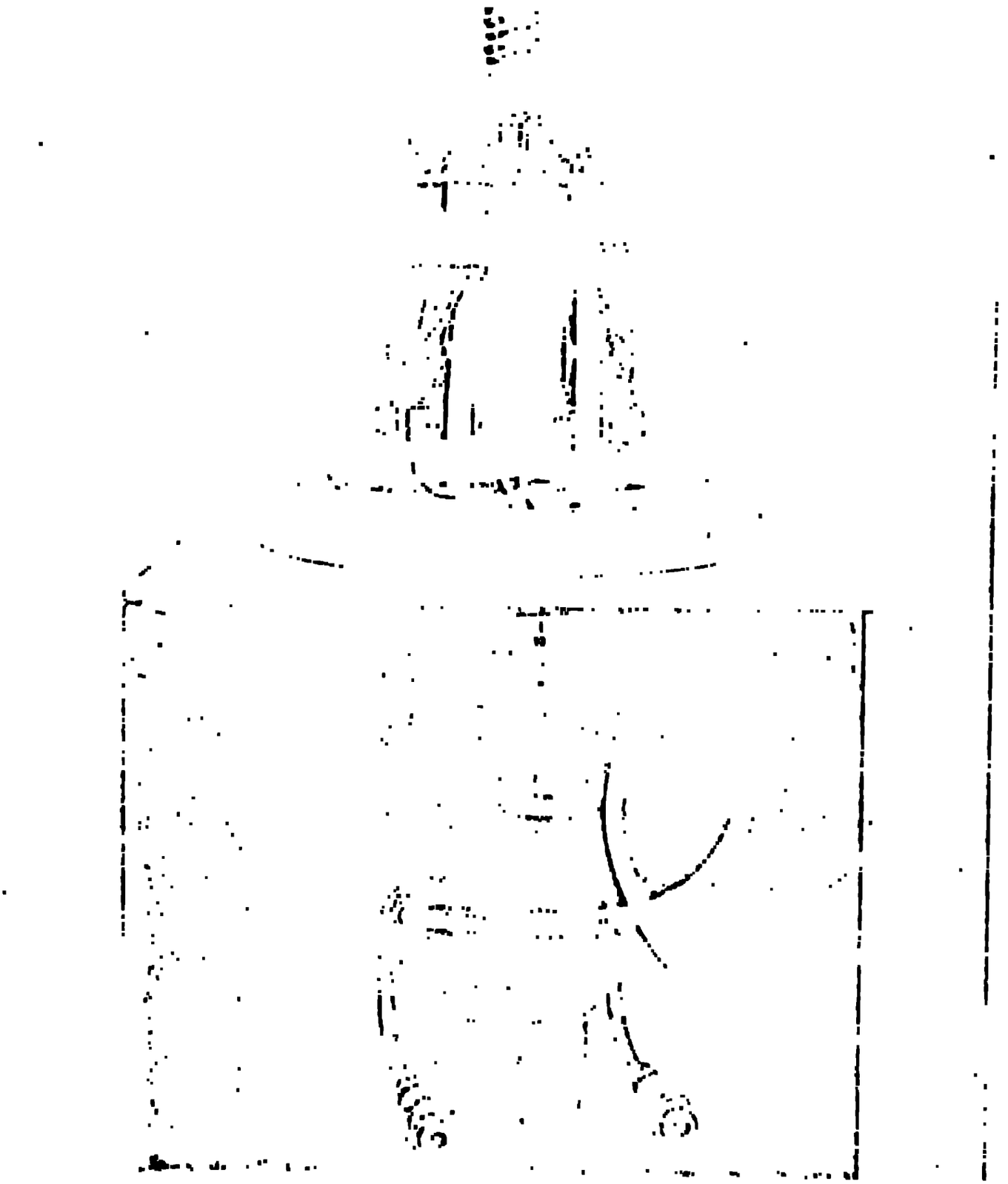

Figure 3. [illegible]

Figure 4. Temperature coefficient plot of Si^+, SiC_2^+, and Si_2C^+ for a typical mass spectrometer Knudsen effusion experiment using a graphite effusion cell with 3×10^{-3} cm^2 orifice area. Dashed lines indicate expected intensity attenuation calculated using Meschi's model for internal gaseous scattering (Ref. 21).

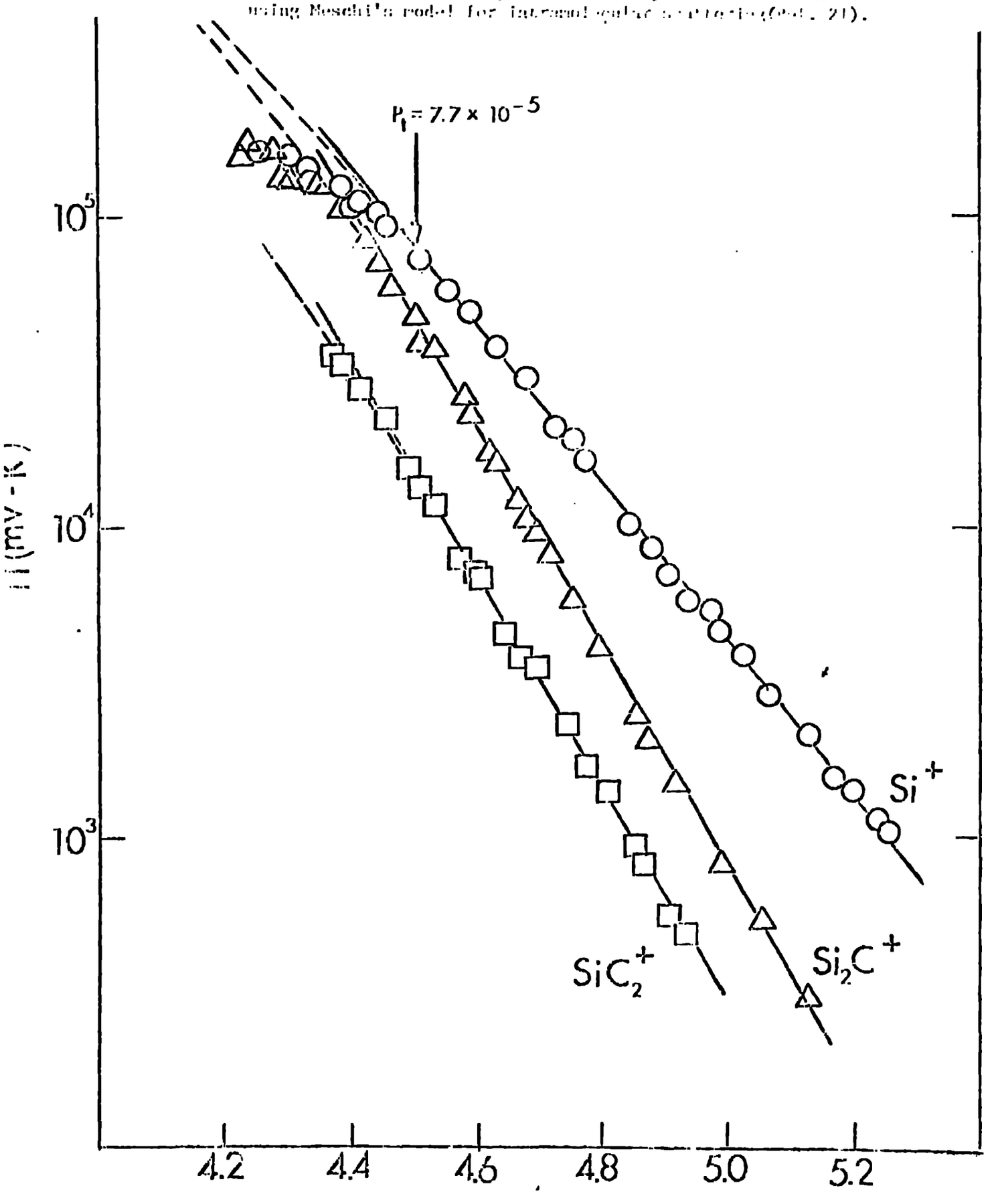

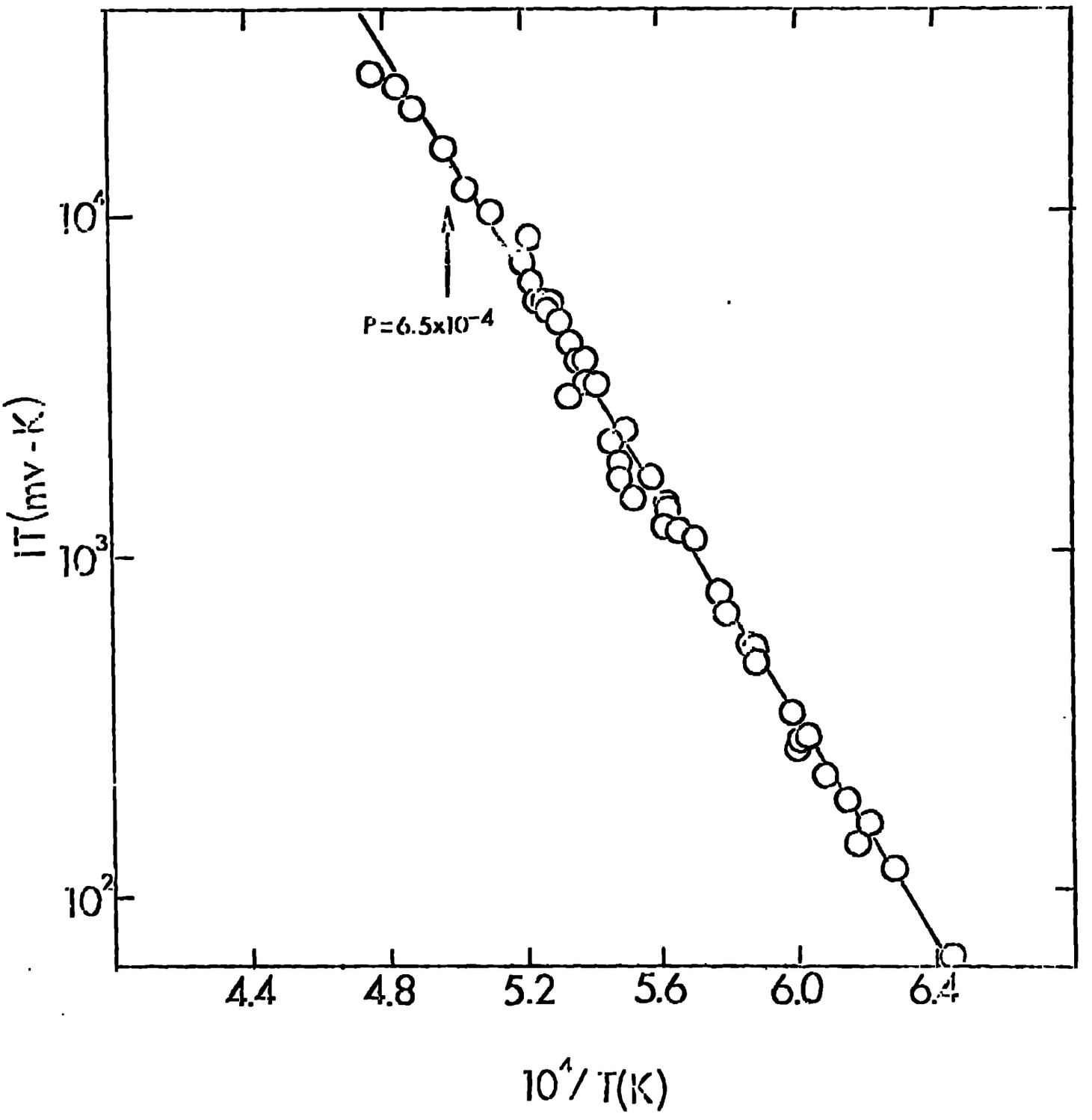

Figure 5. Temperature coefficient plot of Au^+ data from mass spectrometer Knudsen effusion experiment using a graphite effusion cell with 3×10^{-3} cm^2 orifice area.

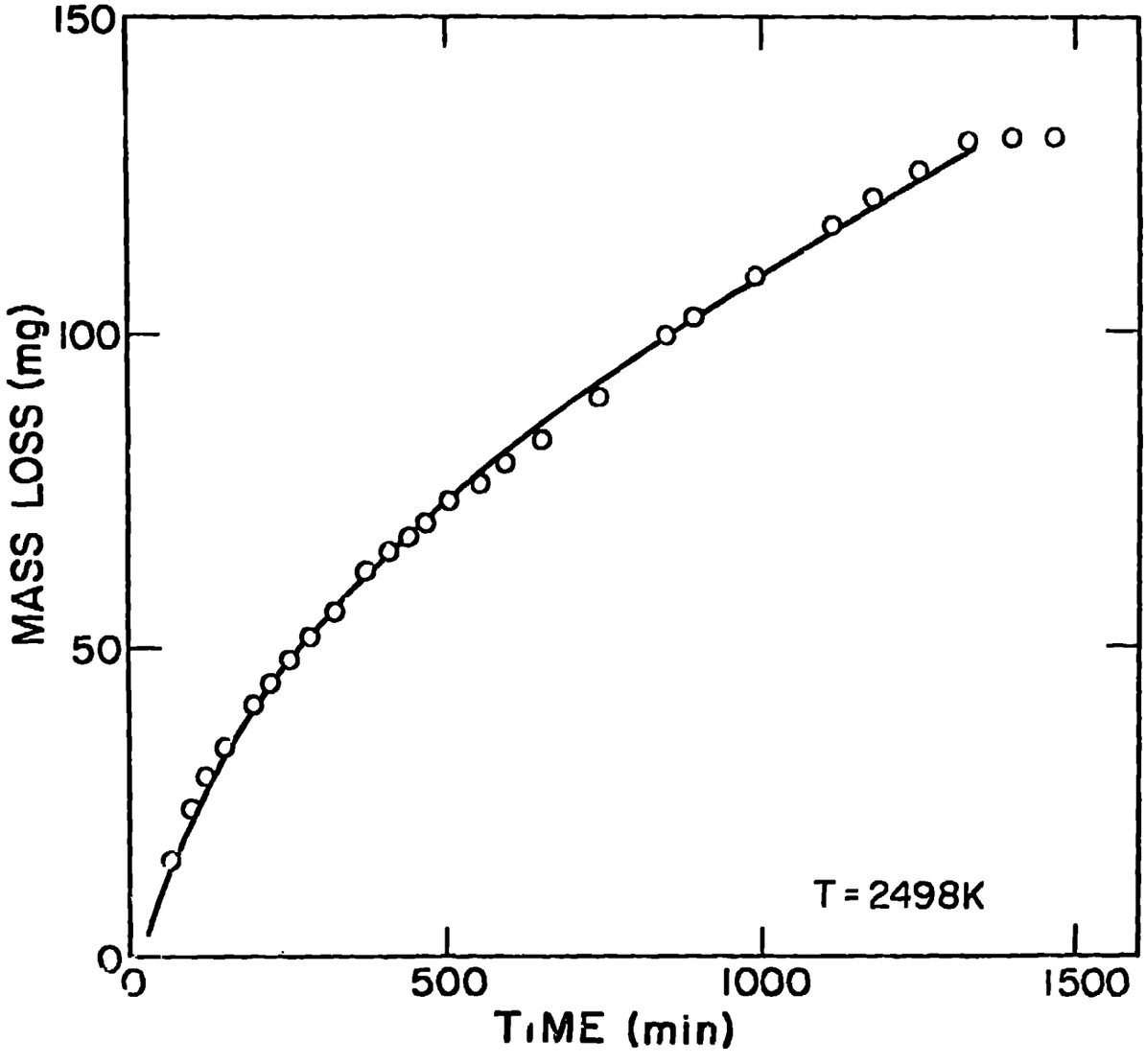

Figure 6. Time-dependence of total mass-loss from a freely vaporizing hexagonal SiC (0001) single crystal face at 2498K.

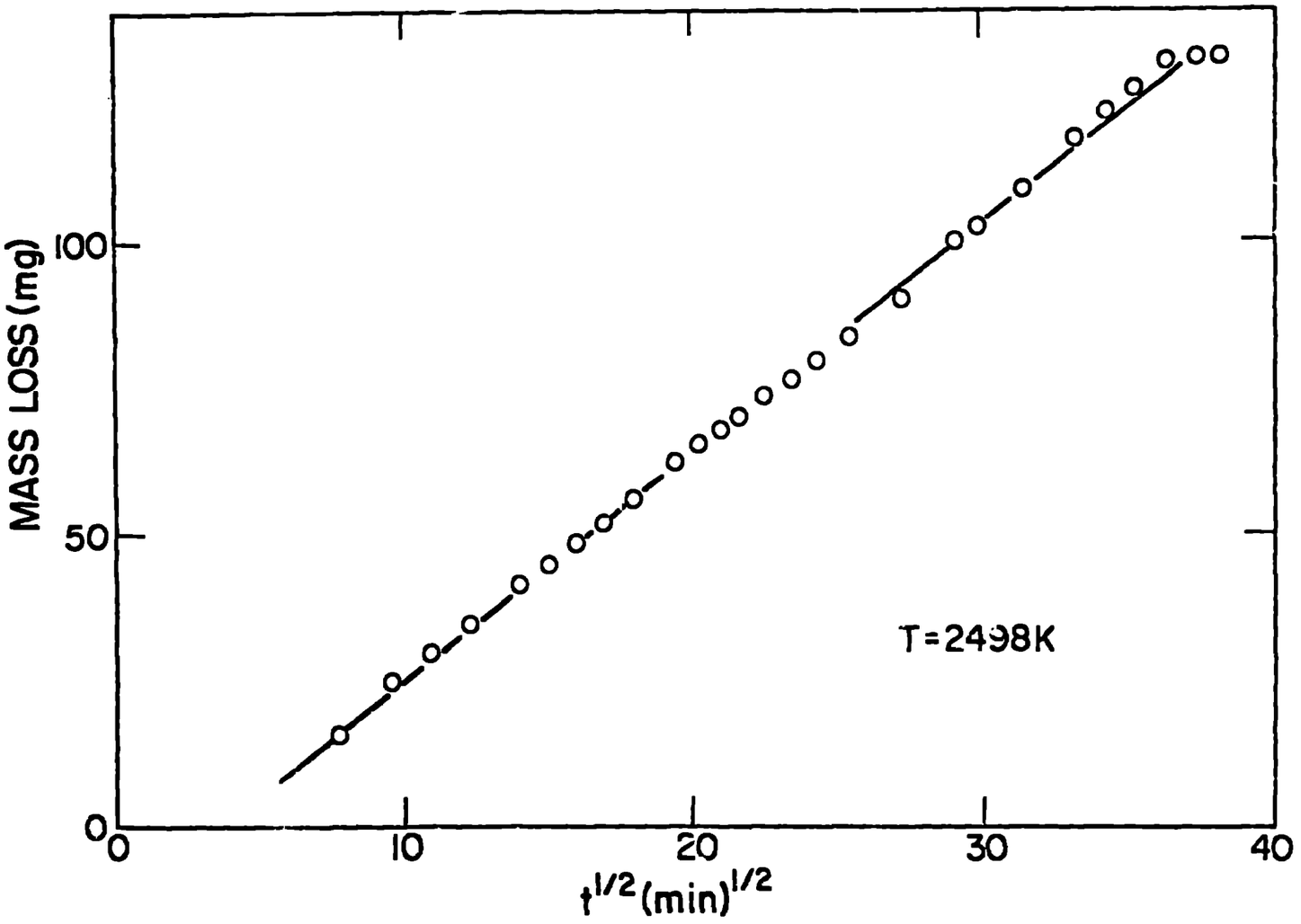

Figure 7. Total mass-loss data of Figure 6 showing parabolic time-dependence.

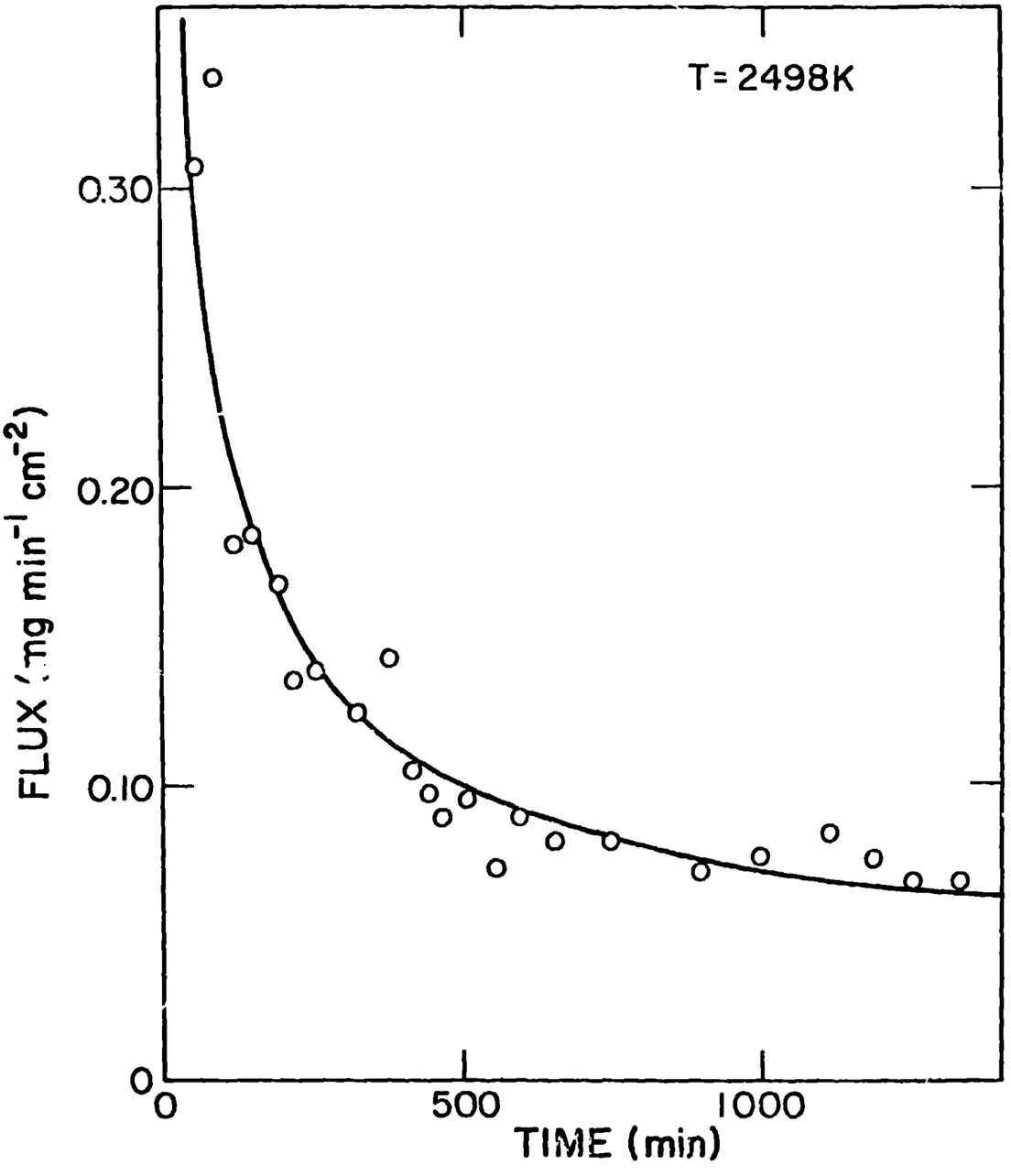

Figure 8. Time-dependence of total flux vaporizing from the (0001) SiC single crystal face at 2498K. Calculated from data in Figure 6.